Distributed phase birefringence measurements based on polarization correlation in phase-sensitive optical time-domain reflectometers

Marcelo A. Soto,[1,*] Xin Lu,[1] Hugo F. Martins,[2] Miguel Gonzalez-Herraez,[3] and Luc Thévenaz[1]

[1]*EPFL Swiss Federal Institute of Technology, Institute of Electrical Engineering, SCI STI LT, Station 11, CH-1015 Lausanne, Switzerland*

[2]*FOCUS S.L., C/ Orellena, 1, 1o Izqda, 28004 Madrid, Spain*

[3]*Departamento de Electrónica, Universidad de Alcalá, Escuela Politécnica DO-231, 28871 Spain*

[*]*marcelo.soto@epfl.ch*

Abstract: In this paper a technique to measure the distributed birefringence profile along optical fibers is proposed and experimentally validated. The method is based on the spectral correlation between two sets of orthogonally-polarized measurements acquired using a phase-sensitive optical time-domain reflectometer (ϕOTDR). The correlation between the two measured spectra gives a resonance (correlation) peak at a frequency detuning that is proportional to the local refractive index difference between the two orthogonal polarization axes of the fiber. In this way the method enables local phase birefringence measurements at any position along optical fibers, so that any longitudinal fluctuation can be precisely evaluated with metric spatial resolution. The method has been experimentally validated by measuring fibers with low and high birefringence, such as standard single-mode fibers as well as conventional polarization-maintaining fibers. The technique has potential applications in the characterization of optical fibers for telecommunications as well as in distributed optical fiber sensing.

OCIS codes: (060.2310) Fiber optics; (060.2270) Fiber characterization; (290.5870) Scattering, Rayleigh; (120.4825) Optical time domain reflectometry.

References and links

1. D. N. Payne, A. J. Barlow, and J. J. R. Hansen, "Development of low- and high-birefringence optical fibers," IEEE Trans. Microw. Theory Tech. **30**(4), 323–334 (1982).
2. V. Ramaswamy, W. G. French, and R. D. Standley, "Polarization characteristics of noncircular core single-mode fibers," Appl. Opt. **17**(18), 3014–3017 (1978).
3. I. P. Kaminow, "Polarization in optical fibers," IEEE J. Quantum Electron. **17**(1), 15–22 (1981).
4. N. Gisin, J. P. von der Weid, and J. P. Pellaux, "Polarization mode dispersion of short and long single-mode fibers," J. Lightwave Technol. **9**(7), 821–827 (1991).
5. J. Noda, K. Okamoto, and Y. Sasaki, "Polarization-maintaining fibers and their applications," J. Lightwave Technol. **4**(8), 1071–1089 (1986).
6. K. Y. Song, W. Zou, Z. He, and K. Hotate, "Optical time-domain measurement of Brillouin dynamic grating spectrum in a polarization-maintaining fiber," Opt. Lett. **34**(9), 1381–1383 (2009).
7. A. J. Rogers, "Polarization-optical time domain reflectometry: a technique for the measurement of field distributions," Appl. Opt. **20**(6), 1060–1074 (1981).
8. J. N. Ross, "Birefringence measurement in optical fibers by polarization-optical time-domain reflectometry," Appl. Opt. **21**(19), 3489–3495 (1982).
9. A. Galtarossa, L. Palmieri, M. Schiano, and T. Tambosso, "Measurements of beat length and perturbation length in long single-mode fibers," Opt. Lett. **25**(6), 384–386 (2000).
10. M. Wuilpart, P. Mégret, M. Blondel, A. J. Rogers, and Y. Defosse, "Measurement of the spatial distribution of birefringence in optical fibers," IEEE Photonics Technol. Lett. **13**(8), 836–838 (2001).
11. A. Galtarossa, D. Grosso, L. Palmieri, and L. Schenato, "Reflectometric measurement of birefringence rotation in single-mode optical fibers," Opt. Lett. **33**(20), 2284–2286 (2008).

#245826 Received 10 Jul 2015; revised 4 Sep 2015; accepted 10 Sep 2015; published 14 Sep 2015

12. A. Galtarossa, D. Grosso, L. Palmieri, and M. Rizzo, "Spin-profile characterization in randomly birefringent spun fibers by means of frequency-domain reflectometry," Opt. Lett. **34**(7), 1078–1080 (2009).
13. L. Palmieri, D. Sarchi, and A. Galtarossa, "Distributed measurement of high electric current by means of polarimetric optical fiber sensor," Opt. Express **23**(9), 11073–11079 (2015).
14. Y. Lu, X. Bao, L. Chen, S. Xie, and M. Pang, "Distributed birefringence measurement with beat period detection of homodyne Brillouin optical time-domain reflectometry," Opt. Lett. **37**(19), 3936–3938 (2012).
15. B. Huttner, J. Reecht, N. Gisin, R. Passy, and J. P. von der Weid, "Local birefringence measurements in single-mode fibers with coherent optical frequency-domain reflectometry," IEEE Photonics Technol. Lett. **10**(10), 1458–1460 (1998).
16. M. E. Froggatt, D. K. Gifford, S. Kreger, M. Wolfe, and B. J. Soller, "Characterization of polarization-maintaining fiber using high-sensitivity optical-frequency-domain teflectometry," J. Lightwave Technol. **24**(11), 4149–4154 (2006).
17. Y. Dong, L. Chen, and X. Bao, "Truly distributed birefringence measurement of polarization-maintaining fibers based on transient Brillouin grating," Opt. Lett. **35**(2), 193–195 (2010).
18. K. Y. Song, "Operation of Brillouin dynamic grating in single-mode optical fibers," Opt. Lett. **36**(23), 4686–4688 (2011).
19. J. C. Juarez and H. F. Taylor, "Polarization discrimination in a phase-sensitive optical time-domain reflectometer intrusion-sensor system," Opt. Lett. **30**(24), 3284–3286 (2005).
20. Y. Koyamada, M. Imahama, K. Kubota, and K. Hogari, "Fiber-optic distributed strain and temperature sensing with very high measurand resolution over long range using coherent OTDR," J. Lightwave Technol. **27**(9), 1142–1146 (2009).
21. H. F. Martins, S. Martin-Lopez, P. Corredera, M. L. Filograno, O. Frazao, and M. Gonzalez-Herraez, "Coherent noise reduction in high visibility phase-sensitive optical time domain reflectometer for distributed sensing of ultrasonic waves," J. Lightwave Technol. **31**(23), 3631–3637 (2013).
22. M. A. Soto and L. Thévenaz, "Modeling and evaluating the performance of Brillouin distributed optical fiber sensors," Opt. Express **21**(25), 31347–31366 (2013).
23. M. Froggatt and J. Moore, "High-spatial-resolution distributed strain measurement in optical fiber with Rayleigh scatter," Appl. Opt. **37**(10), 1735–1740 (1998).
24. W. Li, L. Chen, and X. Bao, "Compensation of temperature and strain coefficients due to local birefringence using optical frequency domain reflectometry," Opt. Commun. **311**(15), 26–32 (2013).
25. L. Palmieri, T. Geisler, and A. Galtarossa, "Effects of spin process on birefringence strength of single-mode fibers," Opt. Express **20**(1), 1–6 (2012).
26. A. E. Alekseev, V. S. Vdovenko, B. G. Gorshkov, V. T. Potapov, and D. E. Simikin, "A phase-sensitive optical time-domain reflectometer with dual-pulse diverse frequency probe signal," Laser Phys. **25**(6), 065101 (2015).

1. Introduction

Birefringence is a property that can be accidentally or intentionally induced in optical fibers and is characterized by the presence of distinct refractive indices for two given orthogonally-polarized lightwaves propagating in the fiber [1–3]. Birefringence can be originated by any kind of factor that breaks the symmetry of the fiber core cross-section [3]; this can be due to imperfections in the manufacturing process or due to external environmental variables. The fiber birefringence is usually not constant along the entire fiber length as a result of non-uniformities in the fiber drawing process. Although the longitudinal birefringence fluctuations resulting from fabrication are typically small, these can be significantly affected by external factors such as temperature and strain, as well as by bends and twists introduced during cabling and installation processes [1,2].

Birefringence limits the data rate capability of optical fibers for telecommunications and therefore it must be kept as low as possible. Although currently manufactured single-mode fibers (SMF) show low levels of birefringence (e.g. $\Delta n \sim 10^{-7}$), small random fluctuations in the core circularity along the fiber (and hence, in the fiber birefringence) can lead to undesired changes in the state of polarization of the propagating light [2,3]. Actually, some short fiber sections can abnormally show large birefringence, being a crucial factor on scaling polarization-mode dispersion (PMD) [1,4], which can significantly distort optical signals and limit the performance of high-speed optical communications systems, especially over long distances.

On the other hand, polarization-maintaining fibers (PMF) are characterized by larger levels of birefringence (e.g. $\Delta n \sim 10^{-4}$), making them very attractive for many applications in telecommunications and optical fiber sensing [5,6]. A high birefringence is a mean to

#245826 Received 10 Jul 2015; revised 4 Sep 2015; accepted 10 Sep 2015; published 14 Sep 2015

maintain a steady state of polarization of the light propagating along an optical fiber well and constantly aligned. Thus, the uniformity of the fiber birefringence is an important parameter for design and system optimization, and any longitudinal variation in the birefringence normally lead to unwanted detrimental effects.

There are many measurement techniques proposed for birefringence measurement; however, most of them only provide an evaluation of the average fiber birefringence, and cannot be used to measure the local birefringence at each fiber position. Only a limited amount of techniques that allow for distributed birefringence measurements have been proposed in the state-of-the-art [7–19]. Considering that the fiber birefringence is affected by external factors, many of those techniques have been exploited for distributed optical fiber sensing in order to detect changes of environmental quantities of interest, such as strain & temperature [6], electric current [13], and external physical perturbations for intrusion detection [19]. These techniques retrieve the information using very diverse approaches, such as polarization-sensitive optical time-domain reflectometry (POTDR) [7–11], polarization-sensitive optical frequency-domain reflectometry (POFDR) [12,13], Brillouin optical time-domain reflectometry (BOTDR) [14], optical frequency-domain reflectometry (OFDR) [15,16], and dynamic Brillouin gratings (DBG) [6,17]. From all these techniques, POTDR and BOTDR are indirect measurement methods, in which the evolution of the state of polarization of the backscattered signal and respective beat length are measured and then used to calculate the local birefringence information based on given mathematical models. On the other hand, OFDR and DBG allow for more direct measurements of the local fiber birefringence. In particular, OFDR has the advantage of providing very high spatial resolutions, however at the cost of a lengthy calculation process. In addition, the optical fiber range that can be measured with the basic OFDR configuration is essentially limited by the coherence length of the used laser. This feature limits significantly the possibilities to characterize long fibers, as typically employed in optical communication systems. In the case of DBG, a complex scheme is typically required: the writing and reading of the grating employing stimulated Brillouin scattering actually uses three high-power lightwaves at different wavelengths, requiring access to both fiber ends and a precise adjustment of frequency and polarization of the interacting waves. While indirect measurement methods allow the characterization of low birefringence fibers, direct methods have only been used for birefringence measurements along PMFs, being impractical (though strictly not impossible [18]) to use them for measuring low birefringence fibers, such as standard SMFs.

In this paper a novel method to directly measure the local birefringence of an optical fiber at any longitudinal position is proposed and experimentally demonstrated. The technique is based on the spectral correlation of phase-sensitive optical time-domain reflectometry (ϕOTDR) measurements under two orthogonal states of polarization. This technique turns out to measure the amount of birefringence present in each fiber section, indifferently to the type of birefringence, which can be linear, circular or even elliptic. In contrast to existing methods, the proposed technique allows a direct characterization of the phase birefringence over very long optical fibers, including not only PMFs (i.e. having a high birefringence) but also fibers that do not necessarily maintain the polarization (i.e. showing low birefringence), such as standard single-mode fibers, dispersion shifted fibers, or dispersion compensating fibers, among many others. The minimum detectable birefringence is highly dependent on the spatial resolution, which defines the spectral width of the obtained correlation peak. In this way, a minimum detectable birefringence of the order of 10^{-7} can be measured for spatial resolutions in the meter range, allowing the characterization of standard single-mode optical fibers.

#245826 Received 10 Jul 2015; revised 4 Sep 2015; accepted 10 Sep 2015; published 14 Sep 2015

2. General concepts

2.1. Principle of conventional ϕOTDR

Conventional ϕOTDR is an accurate and efficient method to measure refractive index variations along an optical fiber [19–21]. The method is based on Rayleigh scattering, which originates in optical fibers from non-propagating density fluctuations in the medium. Rayleigh scattering is an elastic process that induces no frequency shift on the backscattered light.

In the ϕOTDR technique, highly-coherent optical pulses are launched into an optical fiber. As the pulse propagates along the fiber, light is backscattered (through Rayleigh scattering) by randomly and densely spaced scattering centers. This generates a backscattered ϕOTDR signal, whose optical intensity is then measured as a function of time, which in turn is associated with distance. ϕOTDR temporal traces show an optical intensity pattern given by the interference between the multiple Rayleigh randomly backscattered fields; and therefore, the temporal shape of the traces highly depends on the pulse width, the laser optical frequency, and the fluctuating longitudinal refractive index profile. Due to the random nature of the size and relative position of the frozen scattering centers present along an optical fiber, the ϕOTDR temporal traces typically exhibit a noise-like shaped pattern [19–21], as illustrated in Fig. 1. However, despite showing a random shape, this ϕOTDR pattern is static and reproducible for a particular fiber if the measurement conditions do not change in time. However, if the optical path between the scattering centers of a given fiber section varies (e.g. due to changes in the refractive index) between two consecutive measurements, then the ϕOTDR temporal trace will be affected and modified. This working principle is illustrated in Fig. 1.

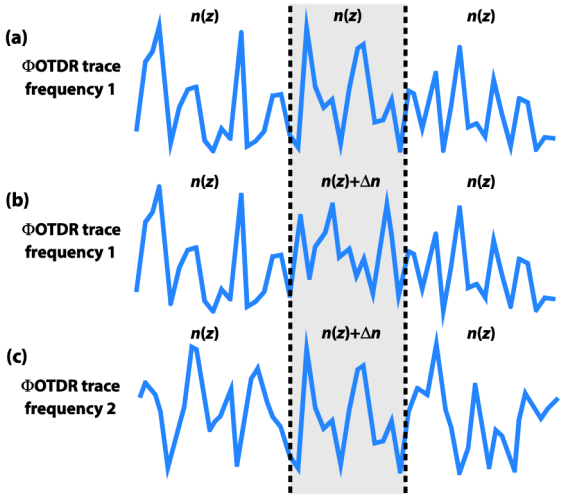

Fig. 1. Principle of conventional ϕOTDR systems. (a) Typical time-domain trace obtained interrogating the fiber (in a given initial state) using pulses with an optical frequency ν. (b) Trace obtained using the same frequency ν, but with the fiber showing a refractive index change Δn in the middle section (note that the traces in (a) and (b) are identical, except in the middle section). (c) The temporal profile of the trace in the central section is retrieved by changing the optical frequency of the probe pulses to $\nu + \Delta\nu$ (note that the central section in (a) and (c) are identical), where the frequency change $\Delta\nu$ is proportional to the refractive index change Δn.

A crucial point for ϕOTDR systems is that if a change Δn in the refractive index occurs uniformly along a fiber section, the temporal profile of the trace corresponding to this section will completely change, as illustrated in the central section of the trace shown in Fig. 1(b).

#245826 Received 10 Jul 2015; revised 4 Sep 2015; accepted 10 Sep 2015; published 14 Sep 2015

However, changes in optical path difference between the scattering centers can be perfectly compensated (in terms of the ϕOTDR outcome) by a shift of the light frequency, so that the original pattern in the fiber section can be exactly retrieved by simply readjusting the light frequency, as shown in Fig. 1(c) (note that the central section of the trace in Fig. 1(c) is the same as in the trace shown in Fig. 1(a)). Under the usual consideration that $\Delta n/n << 1$, the relative frequency detuning required to recover the original trace pattern is exactly equivalent to the relative change in refractive index [20].

Based on this concept, the conventional measurement procedure requires Rayleigh intensity traces to be acquired using different laser frequencies ν, i.e. scanning the light frequency within a given frequency range, so that longitudinal traces measured at a given time t can be allocated in a matrix denoted as $R_t(z,\nu)$. The procedure also needs the use of a reference measurement $R_r(z,\nu)$, which is then cross-correlated in frequency with consecutive Rayleigh measurements $R_t(z,\nu)$ at time t. The cross-correlation $Xcorr(z_0,\Delta\nu) = R_t(z_0,\nu) * R_r(z_0,\nu)$ gives the information of the frequency shift Δν induced by changes in the refractive index in the local Rayleigh reflected spectrum (at a given position z_0) [20]. In other words, the procedure results in a spectrum showing a correlation peak at a frequency shift Δν which is proportional to the local refractive index change Δn. Using this principle, and considering that the refractive index depends on external environmental conditions such as temperature and strain, ϕOTDR systems have been used to perform reliable distributed sensing along many kilometers of optical fiber [20].

2.2. Proposed polarization correlation in ϕOTDR

Compared to the standard ϕOTDR technique, where the polarization state of the interrogating pulse is not a relevant parameter, the method proposed in this paper is based on the correlation of two spectral measurements performed with orthogonal polarization states. It relies on the assumption that the frozen density fluctuations in the fiber scatters light indifferently to its state of polarization, like an ordinary normal reflection on a dielectric medium. For the sake of simplicity, and without loss of generality, the description here will be presented based on the cross-correlation of ϕOTDR traces measured with linear orthogonal states of polarization perfectly aligned to the slow and fast axes of a high birefringence (hi-bi) fiber. However, as it will be described later, many other possibilities could be envisaged to implement the method; this includes the use of the autocorrelation of traces obtained with depolarized light, the cross-correlation of two arbitrary orthogonal states of polarization, etc.

The working principle for the proposed technique is illustrated in Fig. 2. Let us denote the sets of acquisitions at the slow and fast axes as $R_s(z,\nu)$ and $R_f(z,\nu)$, respectively. Since the fiber birefringence imposes a refractive index difference Δn between these two sets of acquisitions, the two local measured spectra (at each fiber location) are expected to be frequency-shifted with respect to each other. Thus, the cross-correlation $Xcorr(z_0,\Delta\nu) = R_s(z_0,\nu) * R_f(z_0,\nu)$, at a given fiber location z_0, will show a spectral peak at a frequency shift $\Delta\nu = \nu_s - \nu_f$, which is proportional to the fiber phase birefringence $\Delta n = n_s - n_f$ [6,17]:

$$n_s(\nu_s)\nu_s = n_f(\nu_f)\nu_f \quad \rightarrow \quad \Delta\nu = \frac{-\nu_f}{n_f^g}\Delta n, \tag{1}$$

where ν_s, ν_f and n_s, n_f are the frequencies and refractive indices along the two orthogonal polarization axes (slow and fast axes), and n^g_f is the group refractive index of the fast axis. Note that due to the finite bandwidth of the system (determined by the pulse width and receiver bandwidth), the correlation peak shows a given non-zero spectral width. This feature combined with the presence of noise in the measurements makes the system require a processing method to retrieve the central frequency of the correlation peak. This can be performed by a single quadratic fitting of the spectral data in the resonance peak [22]. Therefore, the scanning frequency step, the peak spectral width and the signal-to-noise ratio

#245826 Received 10 Jul 2015; revised 4 Sep 2015; accepted 10 Sep 2015; published 14 Sep 2015

(SNR) of the measurements have a direct impact on the uncertainty of the birefringence measurement. Concerning the SNR, there are actually three sources of noise in this system: correlation noise, measurement white noise and thermal drifts of the laser along a measurement sweep (assuming negligible thermal drifts of the fiber along a measurement, as it is the case in our conditions). The measurement white noise can be simply reduced by increasing the number of averaged traces. The drifts of the laser and fiber can be made small by stabilization, making this noise contribution negligible in comparison to the pulse spectral width. On the other hand, correlation noise appears in any phase-OTDR configuration from the spectral correlation between two sets of spectrally-limited measurements showing stochastically distributed amplitudes. This is a common issue in any phase-OTDR system, and not particular of this implementation. The correlation noise can be reduced by increasing the number of spectral points in the measurement [23]. In proper SNR conditions the resolution of the technique is ultimately limited by the width of the correlation peak, which is related to the pulse spectral width.

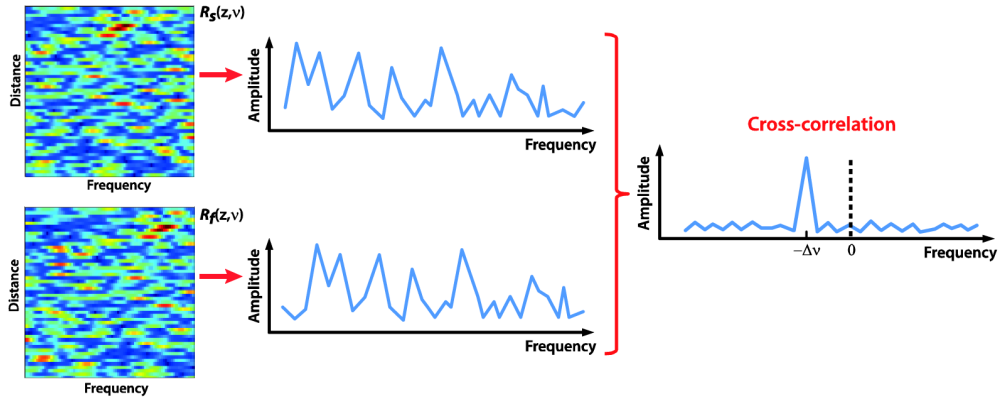

Fig. 2. Principle of the proposed technique to measure the distributed profile of the fiber phase birefringence. The cross-correlation of two local ϕOTDR spectra, measured with orthogonal states of polarization, shows a correlation peak at a frequency shift Δν proportional to the local phase birefringence Δ*n*.

In the case of measuring highly birefringent fibers (e.g. conventional PMFs), the polarization state of the interrogating pulse can be alternately adjusted to match either of the two orthogonal birefringence axes of the fiber. This can be implemented using a polarization switch or any other component (or set of components) that swaps the lightwave polarization between orthogonal linear states. Although the perfect alignment between the polarization of the pulses and one of the axes of the fiber is not essential for the technique, a good alignment is preferred to maximize the amplitude of the polarization cross-correlation peak found at each position along the fiber. Note that this approach is general for any kind of birefringence (e.g. linear, circular or elliptic), and just requires a proper input polarization matching the eigenstates of the fiber. In case of a minor mismatch between the polarization of the incoming light and one of the axes of the fiber, the two measurements are expected to contain slightly correlated information, giving rise to an additional correlation peak at zero-frequency (so-called zero-shift peak [24]). Consequently, the amplitude of the correlation peak at Δν, related to the local birefringence Δ*n,* turns out to be reduced. The amplitude of the correlation peaks at zero-frequency and at Δν will depend on the ratio of light coupled in each of the axes. An elementary analysis based on simple geometrical projections shows that for a mismatch angle θ for the pulse polarization with one of the eigenstate the relative amplitude of the correlation peak at Δν is reduced by a factor $\cos^4\theta$, while the amplitude of the autocorrelation peak grows as $2\sin^2\theta\cos^2\theta$. For instance, if light polarized with an angle of 45° (with respect to the fiber axes) is launched into the fiber, measuring the Rayleigh backscattered light with pulses at two

#245826 Received 10 Jul 2015; revised 4 Sep 2015; accepted 10 Sep 2015; published 14 Sep 2015

orthogonal states of polarization would lead to traces having practically the same information, i.e. highly correlated. This would lead to a strong correlation peak at zero-frequency and an amplitude of the peak at $\Delta\nu$ reduced at 25% of its maximum amplitude. However, as mentioned before, all these impairing effects can be highly mitigated by providing a fairly good alignment between the pulse polarization and one of the axes of the fiber.

3. Experimental setup

For a basic implementation, the proposed technique requires a configuration similar to a standard ϕOTDR [21], with some additional components to enable a precise frequency scanning and to control the polarization of the pulses launched into the fiber. The experimental setup used to validate the method is shown in Fig. 3. The scheme basically requires the generation of an optical pulse having controllable optical frequency (wavelength) and polarization. Pulses with orthogonal polarizations are consecutively launched into the fiber and the respective backscattered Rayleigh signals are acquired in the time domain as a function of the frequency shift of the laser pulses.

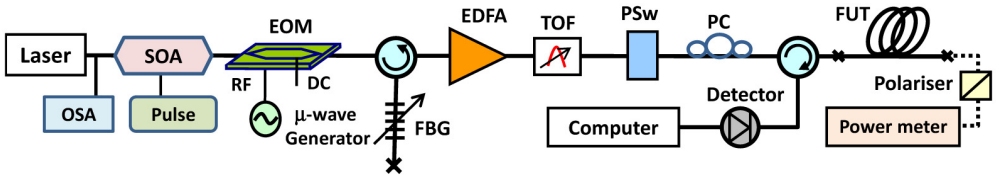

Fig. 3. Experimental setup used to validate the proposed method. OSA: optical spectrum analyzer, SOA: semiconductor optical amplifier, EOM: electro-optic modulator, RF: radio frequency driving voltage, DC: direct current bias voltage, FBG: fiber Bragg grating, EDFA: erbium-doped fiber amplifier, TOF: tunable optical filter, PSw: polarization switch, PC: polarization controller, FUT: fiber under test.

A distributed-feedback (DFB) laser operating at 1535 nm and a semiconductor optical amplifier (SOA) are used to generate optical pulses with high extinction ratio (more than 50 dB). The pulse width is set to 20 ns, corresponding to a spatial resolution of 2 m. Whilst the laser temperature is tuned to coarsely scan the optical frequency of the pulses over a wide frequency range (many tens of GHz), an electro-optic modulator (EOM) driven by a microwave source at several GHz is used to modulate the intensity of the light. A high-resolution (5 MHz bandwidth) optical spectrum analyzer (OSA), self-calibrated on an atomic standard, is used to precisely monitor the coarse laser frequency changes resulting from the temperature tuning, thus providing a precise frequency reference when measuring large frequency ranges, as required for PMFs. In addition the external intensity modulation process gives rise to two sidebands, symmetrically located around the frequency of the incoming light (i.e. around the emitted laser frequency), which can be accurately and finely scanned with steps of 10 MHz by simply changing the frequency of the microwave source. Considering that the light launched into the fiber requires a single frequency component, a tunable narrowband fiber Bragg grating (FBG) is utilized to select one of the sidebands generated by the EOM. Optical pulses are then amplified by an Erbium-doped fiber amplifier (EDFA), followed by a tunable optical filter (TOF) used to suppress the amplified spontaneous emission generated by the optical amplifier. Before launching the pulses into the fiber under test (FUT) through a circulator, a polarization switch (PSw) and a polarization controller (PC) are used to launch light into the FUT with orthogonal states of polarization. Whilst the function of the polarization controller is to align the polarization of the pulses with one of the polarization axes of the fiber, the polarization switch changes the polarization of the light from a given state to the orthogonal one. Note that the polarization alignment carried out by the polarization controller is only necessary for optimization when measuring high birefringence fibers, where the two orthogonal axes are clearly defined. As it will described

#245826 Received 10 Jul 2015; revised 4 Sep 2015; accepted 10 Sep 2015; published 14 Sep 2015

below, this part of the scheme can be completely skipped when measuring low birefringence fibers such as SMFs, since there is no clear polarization alignment to make in such fibers. At the output of the FUT, a polarizer and a power meter have been used to ensure an optimized polarization alignment in the PMFs. These components are actually not essential for the technique, but they are helpful for optimizing and monitoring the polarization alignment.

At the receiver end, Rayleigh backscattered signals are directed into a 125 MHz bandwidth photo-detector, and the corresponding time-domain traces are acquired and processed by a computer.

4. Experimental results and discussions

4.1. Birefringence measurements along polarization-maintaining fibers

The most-basic measurement procedure requires the consecutive acquisition of traces along the two orthogonal polarization axes of the fiber. After performing a standard set of ϕOTDR measurements at a given polarization, a second set of traces is acquired using pulses with orthogonal polarization. Using the setup depicted in Fig. 3, Rayleigh backscattered traces have been measured for two distinct PMFs: a 90 m Panda and a 100 m elliptical-core fiber. The optimized polarization alignment to the slow and fast axes of the PMFs has been realized as described in the previous section. Thus, maximizing (or minimizing) the monitored power ensures a maximum coupling of light into the slow (or fast) polarization axis (in this case the polarizer placed at the fiber output is aligned to the slow axis of the PMF). This way the correlation peak amplitude is enhanced, resulting in measurements with low frequency uncertainty. As mentioned in Section 3, in order to scan a wide frequency range (larger than the EOM bandwidth) the laser frequency has been coarsely tuned changing the laser temperature, while the resulting absolute frequency changes are monitored in the OSA with a resolution of 5 MHz. Thus, combining this coarse tuning with the fine frequency shift induced by the external modulation, a precise scanning over a wide frequency range (in the order of several tens of GHz) could be achieved.

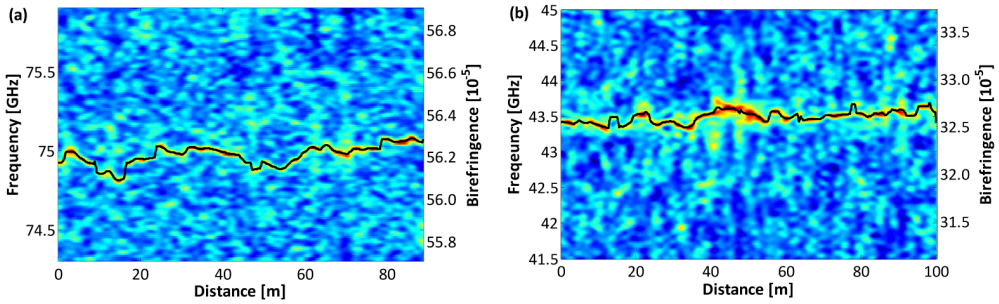

Fig. 4. Distributed profile of phase birefringence versus distance along (a) a 90 m Panda PMF and (b) a 100 m elliptical-core PMF. Left-hand side vertical axis: Measured frequency. Right-hand side vertical axis: Birefringence value calculated using Eq. (1).

Figure 4 shows the distributed profile of the birefringence-induced frequency shift (left vertical axis) as a function of distance, obtained by correlating Rayleigh spectral measurements along the two orthogonal states of polarization for the Panda (Fig. 4(a)) and elliptic-core (Fig. 4(b)) fibers. Fitting the correlation peak spectrum with a quadratic curve [22], the correlation frequency profile has been obtained as a function of the distance. Using this correlation frequency profile $\Delta\nu(z)$ and Eq. (1), the distributed profile of the local phase birefringence $\Delta n(z)$ has been retrieved, as shown by the right-hand side vertical axis of the figures. The depicted experimental results validate the proposed method, which provides clear measurements of non-uniform phase birefringence along both optical fibers when using 2 m spatial resolution.

#245826 Received 10 Jul 2015; revised 4 Sep 2015; accepted 10 Sep 2015; published 14 Sep 2015

Considering that the measurement time with ϕOTDR can be of the order of a few seconds for such short fibers, temperature drifts and laser frequency fluctuations during the acquisition time could be expected to induce frequency errors that can likely reach a few tens of MHz. In the case of measuring fibers with high birefringence, this would represent an error lower than 1% of the absolute measured frequency (being of the order of tens of GHz). For some kinds of applications this low level of error can be tolerated; however, if higher precision is required, a correction method based on the measurement of the zero-shift correlation peak could be used to compensate undesired cross-sensitivities, such as fiber temperature changes and/or laser frequency drifts. This would provide higher robustness to the system and higher reliability to the measurements.

As an alternative measurement process, one might actually think about the possibility of acquiring a single set of measurements, while launching light polarized with an angle of 45° with respect to the fiber axes. This way, the two orthogonal polarization axes of the fiber can simultaneously propagate light, enabling the birefringence information to be retrieved from the auto-correlation of a single measured spectrum at each position. This procedure has actually been tested experimentally, giving similar results to the ones shown in Fig. 4; however, lower measurement contrast was obtained in the correlation peak, leading therefore to slightly noisier measurements.

At this stage it is worth mentioning that the broad frequency scanning required by the large birefringence of PMFs (typically covering ranges of some tens of GHz) can be partially avoided if the average fiber birefringence and associated frequency shift are approximately known. In such a case it is possible to scan distinct narrow spectral regions for the two sets of measurements; with a frequency separation equal to the expected average frequency difference. However, based on Eq. (1), special attention should be paid to the polarization alignment in this case, so that pulses at higher optical frequency enter in the fast axis of the PMF, while the lower frequency pulses must be aligned to the slow axis. Then, the data processing should simply take into account the frequency difference between the two scanned ranges. For instance if the expected average frequency shift associated to the average birefringence is 40 GHz, then traces along the two polarizations can be acquired by scanning only over some hundreds MHz or a few GHz in two independent spectral regions separated by 40 GHz. Thus, if under this condition the cross-correlation spectrum shows a peak at $\Delta\nu'(z_0)$ at a given position z_0, then the real frequency $\Delta\nu(z_0)$ associated to the birefringence $\Delta n(z_0)$ has to be calculated as $\Delta\nu(z_0) = 40\ \text{GHz} + \Delta\nu'(z_0)$. Incidentally, the technique can also identify the slow and the fast fiber birefringence axis unambiguously. As in the previous case, in this approach a precise control or monitoring of the absolute optical frequency is required to avoid large uncertainty in the measured birefringence, by applying the same above described experimental procedure depicted in Fig. 3. Results show similar behaviors, within a ± 5 MHz uncertainty given by the bandwidth resolution of the OSA.

4.2. Birefringence measurements along standard single-mode fibers

So far the proposed method has been described and experimentally validated using high birefringence fibers; however, the technique can also be employed to measure low birefringence values along standard SMFs.

Unlike hi-bi fibers, in low birefringence fibers the polarization of the incoming light changes randomly during propagation and, in general, can never be made aligned to any particular axis. Thus, as a result of the random fluctuations of the polarization state of the pulses, the two sets of measurements will contain highly correlated information, giving rise to a correlation peak at zero frequency (the zero-shift peak). In addition, another correlation peak containing information about the birefringence is expected, which randomly and alternately changes between $\Delta\nu$ and $-\Delta\nu$ according to the local phase matching condition. Note that, although the state of polarization (SOP) of the pulse evolves randomly along the fiber and may not always be aligned with the principal axes of the fiber, it can always be

#245826 Received 10 Jul 2015; revised 4 Sep 2015; accepted 10 Sep 2015; published 14 Sep 2015

decomposed into an orthogonal combination of light in two local eigenstates of the fiber, both of them showing a maximal effective index difference. Therefore, the frequency offset values ($\Delta\nu$ and $-\Delta\nu$) recovered from the cross-correlation diagram correspond to the magnitude of the fiber birefringence, regardless of its type and orientation. Indeed, the only effect of the varying SOP orientation will be related to the height of the correlation peaks. The local amplitude of these peaks depends on the ratio of light coupled into the slow/fast axis at each fiber location. Combined with measurements performed for several input SOPs, this feature could be eventually used to retrieve the orientation of the birefringence vector. Eventual alternatives to retrieve the absolute angle of the birefringence vector require further extensive investigations going beyond the scope of this paper. Note that the locally measured frequency shift $\Delta\nu$ corresponds to a measurement of the local birefringence Δn between the local eigenstates of polarization, indistinctively to the type of birefringence (linear, circular or elliptic). This feature can be seen as an intrinsic limitation to the technique, which cannot at this stage distinguish between these different types of birefringence.

To better evaluate the capability of the proposed technique to measure low birefringence, old SMFs have been used in our experiment. In particular, to avoid fast rotations of the birefringence axes [25] (compared to the spatial resolution of 2 m) unspun SMFs drawn in the mid 1980's have been used in this case. Since SMFs do not have maintained polarization axes, it is not worth performing any polarization adjustment in this case; however, measuring with two orthogonal states of polarization is still essential to obtain the birefringence information along the fiber.

Figure 5 shows the measured frequency shift along a 3 km-long SMF, when using 2 m spatial resolution, 1000 averages and a scanning frequency step of 10 MHz. As expected, the resulting correlation spectrum shows three correlation peaks, one at zero frequency and two peaks at $\pm\,\Delta\nu$. The absolute value of the birefringence profile along the fiber can be retrieved from any of the two peaks at $\pm\,\Delta\nu$. It is interesting to notice that clear variations of the local birefringence, being in the order of 10^{-6}, can be precisely measured along the entire fiber length.

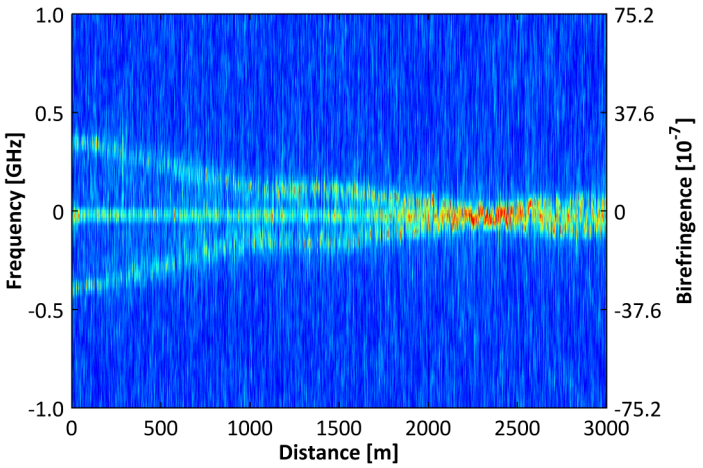

Fig. 5. Distributed profile of phase birefringence versus distance along a 3 km-long SMF, obtained from the cross-correlation of two consecutive Rayleigh measurements at orthogonal polarizations. Left-hand side vertical axis: Measured frequency. Right-hand side vertical axis: Birefringence value calculated using Eq. (1).

Note that the zero-shift correlation peak obtained in Fig. 3 is actually equivalent to the one obtained in the standard ϕOTDR system [20] used for temperature and strain sensing, and therefore provides information about fiber temperature and strain variations during the acquisition time (~40 s), as well as about the average laser frequency drift. If any of these

#245826 Received 10 Jul 2015; revised 4 Sep 2015; accepted 10 Sep 2015; published 14 Sep 2015

factors changes during the acquisition of the two states of polarization, the correlation peaks at ± Δν containing the birefringence information will drift together with the zero-shift correlation peak, introducing an offset in the frequency measurements [24]. A small negative offset can actually be observed in Fig. 5. After applying a fitting process to retrieve the birefringence-induced frequency shift from one of the side correlation peaks and correct its value by the offset indicated by the zero-shift correlation peak frequency, a reliable birefringence profile along the optical fiber can be obtained. However, in order to simplify the data processing required to retrieve the longitudinal birefringence profile and to further mitigate the detrimental impact of laser frequency fluctuations and temperature drifts during the measurement process, alternative acquisition procedures can be implemented. This will be discussed in the next section.

4.3. Alternative scheme for measuring low birefringence levels

Although Fig. 5 demonstrates the ability of the method to properly retrieve the longitudinal birefringence profile of standard SMFs, more robust and precise measurements can be obtained by acquiring simultaneously the Rayleigh traces with orthogonal states of polarization. For this purpose, an important modification to the setup reported in Fig. 3 has to be made: this consists in removing the polarization switch and polarization controller in front of the FUT and inserting a block to generate two phase-decorrelated (incoherent) pulses with orthogonal polarizations at the same optical frequency (this block will be described later in Fig. 6, and as mentioned below, it can also be placed before shaping the pulses launched into the fiber). Thus, launching the resulting depolarized pulse into the FUT, Rayleigh traces containing the information from the two orthogonal axes of polarization can be simultaneously acquired, so that the useful birefringence information can be retrieved by the auto-correlation of the measured local spectrum. Under this condition the auto-correlation of the local spectrum is expected to give rise to a strong correlation peak at zero frequency and two identical peaks symmetrically placed at frequencies ± Δν [16,24]. Note that, whilst the orthogonal polarizations ensure the excitation of both axes of the fiber, the incoherence of the light ensures the non-interfering propagation of the two pulses along the fiber. It is worth mentioning that if the two pulses are coherently launched into the fiber, this simply results in a change of the pulse polarization, being equivalent to use a single pulse with the resulting state of polarization, just like a standard ϕOTDR. In such a situation, changes in the light polarization inside the fiber might lead to local polarization states perfectly aligned to one of the fiber axes, so that traces will contain information of a single polarization axis at that given location, thus leading to an auto-correlation spectrum showing no peak at ± Δν. Thus, launching two incoherent pulses simultaneously into the fiber secures the combined measurement of two independent orthogonal polarization channels, thus increasing the accuracy of the measured birefringence.

In order to generate the two incoherent pulses with orthogonal polarizations, two different schemes have been implemented, as shown in Fig. 6. These two schemes essentially depolarize a continuous-wave light, and therefore a simple implementation is to place them before shaping the pulses in the system.

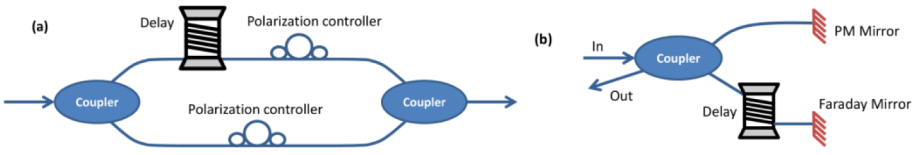

Fig. 6. Possible implementations to generate two incoherent lightwaves (having the same frequency) with orthogonal polarizations. (a) Scheme using an unbalanced Mach-Zenhder interferometer. (b) Scheme using a polarization-maintaining mirror and a Faraday mirror.

#245826 Received 10 Jul 2015; revised 4 Sep 2015; accepted 10 Sep 2015; published 14 Sep 2015

Figure 6(a) shows a scheme in which the incoming light is split into two branches: one of them rotates the polarization of the light by 90° with respect to the other branch. Additionally, a delaying element (given by a long optical fiber) has to be placed in one of the branches to cause a delay longer than the coherence time of the optical source. Then, an optical coupler is used to recombine the light from the two branches. The second implemented scheme is depicted in Fig. 6(b), where the incoming light is divided into two beams by a polarization-maintaining coupler having four ports: a fraction of the light is reflected by a polarization-maintaining mirror, while the other fraction is reflected by a Faraday mirror, which rotates the polarization in 90°. A delaying element is also necessary, placed in any of the two branches but preferably in that containing the Faraday mirror that maintains the orthogonality all along the back propagation. The orthogonally-polarized waves reflected from the mirrors are combined and exit through the fourth port of the coupler. An important issue is that the power levels of both branches (in the two schemes) have to be precisely equalized to make the depolarization of the resulting pulses perfect. Thus, using any of these configurations, the Rayleigh light reaching the detector would contain a linear incoherent superposition of the traces for the two orthogonal polarizations. This means that a single measurement is sufficient to get all information from the Rayleigh backscattered light, while the local birefringence along the fiber can be retrieved from the auto-correlation of the measured spectrum at each fiber location.

It has been experimentally verified that both schemes in Fig. 6 provide practically the same performance. Figure 7 shows the distributed spectrum obtained by auto-correlating a single measurement in the improved configuration. Whilst the spectrum obtained with the basic implementation (reported in Fig. 5) show intervals with clear null (fading) response of the correlation peaks at $\pm \Delta\nu$ (with responses alternating between the two bands), the spectrum obtained with the two simultaneous polarizations (see Fig. 7) shows no long sections with deep correlation fading. However, it is possible to observe that the correlation peaks in the latter case could also partially vanish and/or broaden within short fiber sections, which has been attributed to fast variations of the fiber birefringence axes within the given spatial resolution (2 meter) of the system. It is important to mention that due to these fast birefringence variations at some specific fiber locations, it was not always possible to find the correlation peak frequency by a simple fitting process. For this reason a black line indicating only the average birefringence variations along the fiber has been included in the figure. This curve has been obtained using a moving average of the peak frequency obtained by a quadratic fitting, using a window of 50 points, thus representing the average value along 10 m of fiber. The only purpose of this curve is to help the reader to better visualize the evolution of the birefringence along the fiber, and has not the intention of showing the birefringence profile with the spatial resolution of 2 m. In order to obtain precise birefringence measurement following the fast variations shown in Fig. 7, a dedicated scheme for cm-resolution should be implemented. This kind of implementation needs further work and goes beyond the scope of this paper.

#245826 Received 10 Jul 2015; revised 4 Sep 2015; accepted 10 Sep 2015; published 14 Sep 2015

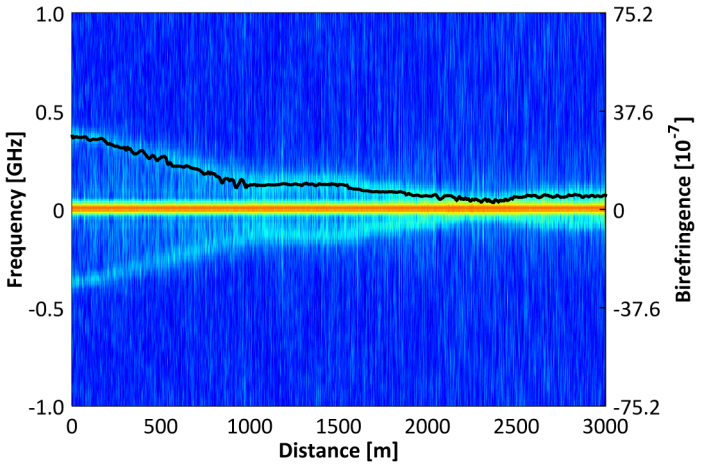

Fig. 7. Distributed profile of phase birefringence versus distance along a 3 km-long SMF, obtained from the auto-correlation of a single Rayleigh measurement containing the information of the two orthogonal states of polarizations. Left-hand side vertical axis: Measured frequency. Right-hand side vertical axis: Birefringence value calculated using Eq. (1).

4.4. Minimum detectable birefringence

The lowest birefringence value being measured by the system is determined by all factors impacting on the frequency accuracy of the measurements. Considering that the impact of noise in the ϕOTDR temporal traces can be arbitrarily reduced by averaging, that the correlation noise can also be reduced by increasing the measured spectral span, and that the laser and fiber temperature drifts along the fiber are negligible over the time of a measurement (typically 40 seconds), the resolution turns out to be ultimately given by the pulse spectral width. By similarity, a conservative limit inspired by the Rayleigh criterion for the resolving power of any optical system can be applied, stating that the best measurable birefringence is ultimately limited by the correlation peak width. Considering 20 ns Gaussian-shaped pulses, the theoretically expected full-width at half-maximum (FWHM) of the correlation peaks is about 44 MHz [26], being in good agreement with the experimental width shown in Fig. 8(a). This actually corresponds to a minimum measurable birefringence of $\sim 3 \cdot 10^{-7}$ and a polarization beat length of about 5 m, thus ensuring that the spatial resolution is still a fraction of the beat length. The spectral width of the correlation peak can be actually further reduced in order to increase the precision in the retrieved birefringence; however this must be traded off with the use of longer spatial resolutions, as illustrated in Fig. 8(b). This figure actually depicts the FWHM of the correlation peaks as a function of the spatial resolution, showing a good agreement between the expected theoretical predictions and experimental results. Furthermore, it is important to mention that when long pulses are used, the correlation peak spectral width is ultimately given by the linewidth of the light source. This is actually the limitation imposed by the laser coherence length to the longest pulse width allowed in ϕOTDR systems.

#245826 Received 10 Jul 2015; revised 4 Sep 2015; accepted 10 Sep 2015; published 14 Sep 2015

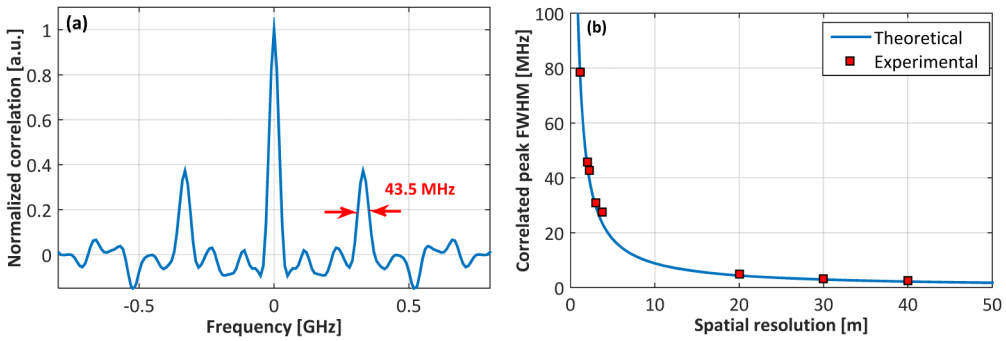

Fig. 8. Impact of the pulse duration on the FWHM of the correlation peaks at ± Δν, when using Gaussian-shaped pulses. (a) Correlation spectrum obtained at a position of 200 m (in the 3 km-long SMF reported in Fig. 7), using a 2 m spatial resolution. (b) Correlation peak spectral width as a function of the spatial resolution. Theoretical estimations (straight blue line) are compared with experimental values (red squares).

5. Conclusion

A technique that measures the distributed phase birefringence profile along optical fibers has been proposed and experimentally validated. The method makes use of the spectral cross-correlation between two orthogonally-polarized ϕOTDR measurements and offers the possibility to discriminate local birefringence variations along many tens of km of optical fibers with metric spatial resolution. The high birefringence accuracy demonstrated (in the order of $\sim 10^{-7}$) enables a proper characterization of low birefringence single-mode fibers.

As described here the method cannot discriminate between linear and circular polarization, which can be experienced like an intrinsic limitation. However, it should be noted that this discrimination is theoretically not impossible, though requiring extensive developments and, unlike some of the previous proposals in the literature, our method provides a direct measurement of the fiber phase birefringence. It can indistinctively measure any kind of birefringence –linear, circular or even elliptic– since the scheme does not include any polarization selective element and can be implemented with depolarized light. Moreover, the technique is simple to deploy and requires relatively low average power levels, while providing good signal-to-noise ratio. The same method can be used to characterize both high birefringence fibers as well as low birefringence single-mode fibers. Beyond the telecom domain, this method could be extremely useful in optical fiber sensing, particularly for sensing any kind of physical quantity affecting the phase birefringence of the fiber.

Acknowledgments

This work was performed in the framework and with the support of the COST Action TD1001 OFSeSa. M. A. Soto and L. Thévenaz acknowledge the support of the Swiss State Secretariat for Education, Research and Innovation (SERI) through the project COST C10.0093. MGH acknowledges support by the European Research Council through Starting Grant U-FINE (Grant no. 307441), by the Spanish Ministry of Science and Innovation under Project TEC2012-37958-C02-01, the INTERREG SUDOE program ECOAL-MGT and the Comunidad de Madrid under project SINFOTON-CM:S2013/MIT-2790. HFM acknowledges funding through the FP7 ITN ICONE program, gr. #608099, funded by the European Commission.